Acta Translational Medicine *An International Scientific Journal*	ISSN: 2521-8662	Volume 1	Issue 2	pp.7-12	June 2019

DIFFERENTIAL DIAGNOSIS OF BENIGN PROSTATE LESIONS AND PROSTATIC CANCER USING MONO-EXPONENTIAL, BI-EXPONENTIAL MODELS BASED DIFFUSION WEIGHTED IMAGING

Jie Zhang[#], Hai-dong Chen[#], Li-fen Xie[#], Fen-xiong Liang, Yong-jun Peng[*], Jun Mao[*]

Department of Radiology, Zhuhai People's Hospital (Zhuhai hospital affiliated with Jinan University), Zhuhai 519000, China

[*]*Corresponding E-mail: Yong-jun Peng MS, sxpj2196@163.com*
Jun Mao, maoj2005@126.com
[#]*Equal contributors: Jie Zhang, Hai-dong Chen, and Li-fen Xie contributed equally to this work.*

Abstract: Objectives: To evaluate and compare the value of various metrics obtained from mono-exponential model (MEM) and bi-exponential model (BEM). MEN and BEM was based on diffusion weighted imaging (DWI) in differential diagnosis of benign and malignant prostate lesions. Methods: Consecutive 124 patients with pathologically confirmed prostate lesions (4 patients were confirmed prostatitis,43 patients were confirmed Benign prostatic hyperplasia,30 patients were confirmed prostatitis with hyperplasia, 47 patients were confirmed prostatic cancer) received DWI of MEM and BEM. The Apparent diffusion coefficient (ADC) from single b-factor range DWI were compared with the ADC_{slow}, ADC_{fast}, $ADC_{standard}$ and F_{fast} from extended b-factor range DWI imaging between benign and malignant group. Receiver operating characteristic（ROC）curve and One Way ANOVA were performed to evaluate the diagnostic performance of different parameters. Results： The mean and normalised ADC_{slow}, ADC_{fast}, F_{fast} and ADC values were significantly lower in malignant group than those in benign group ($P < 0.05$). $ADC_{standard}$ was significantly higher in malignant group than those in benign group ($P < 0.05$). If the maximum Youden's index was taken as an optimal cut-off, the diagnostic threshold of ADC_{slow}, ADC_{fast}, $ADC_{standard}$, F_{fast} and ADC was 0.350×10^{-3} mm^2/S, 0.520×10^{-3} mm^2/S, 4.95×10^{-3} mm^2/S, 0.421, 1.05×10^{-3} mm^2/S, respectively. Conclusion: Different models of DWI, including MEM and BEM are useful in the differential diagnostic of the benign and malignant prostate lesions. However, ADC_{slow}, ADC_{fast}, F_{fast} have better diagnostic performance with increased sensitivity and specificity.

Key words: Prostate cancer; Prostate lesions; Diffusion magnetic resonance imaging; Diffusion weighted imaging

INTRODUCTION

Prostate lesions such as Benign Prostatic Hyperplasia and prostatitis which are common in genitourinary system of men. And the rate of prostatic carcinoma increased year by year. Diffusion weighted imaging (DWI) is a noninvasive functional MRI technique that provides information on the Brownian motion of water molecules. Malignant tumors can be detected because of its higher cellular density, which limits the diffused motion of water molecules. So DWI can be used to do differential diagnosis between the benign and malignant prostate lesions. Study of the apparent diffusion coefficient (ADC) value obtained which

based on only two b-values (usually 0 and 800 s/mm^2 in the pelvis) is usually used to evaluate the restriction of water diffusion [1]. The ADC value has limited specificity in the diagnosis of prostate lesions, because it can only reflect water diffusion behavior. The microcirculation of blood in the capillary network could not be reflected. IVIM (intravoxel incoherent motion) imaging is a method based on bi-exponential model that reflects the ADC value from two components: perfusion and diffusivity [2]. The parameters calculated from the IVIM have been used to assess organ properties [3], including diffusion coefficient (ADC_{slow}), pseudo-diffusion coefficient (ADC_{fast}), standard coefficient ($ADC_{standard}$) and perfusion fraction (f) [4]. The aim of our study was to objectively compare the parameters (ADC_{slow}, ADC_{fast}, $ADC_{standard}$, and f) obtained from multi-b-values of IVIM and the parameter (ADC) from mono-exponential model DWI on prostate benign lesions and malignant tumors. In addition, the efficacy of these parameters were evaluated separately.

METHODS

Data sources and search methods

From January, 2009 to September, 2018, patients who underwent conventional diffusion weighted MRI (b = 0,1000 s/mm^2) and IVIM (b = 0-1000/mm^2) were included. All the patients were proved as prostate diseases by pathology. The exclusion criteria were as follows: (1) prior therapy for PCa before MRI; (2) poor images quality due to movement artifacts, magnetic susceptibility artifacts, or implants in the hip; (3) the previous biopsy performed within eight weeks before the MRI. The histopathologic analysis of the prostate after examination was performed. Finally, one hundred and twenty four patients who had been diagnosed as benign and malignant prostate lesions were recruited for this retrospective study (Fig.1), including cancer (n = 47), Benign Prostatic Hyperplasia (n = 4), prostatitis (n = 4) and prostatitis with hyperplasia (n = 30).

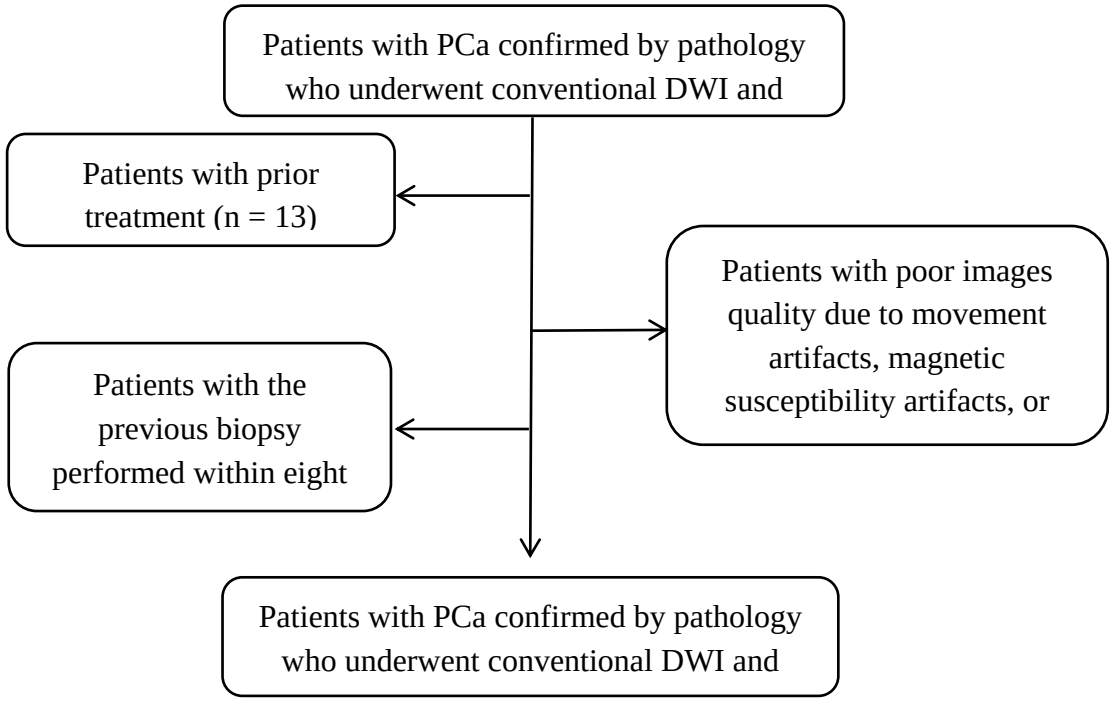

Fig.1 Flowchart of patient selection.

MRI examination

All patients received examination on a 3T MRI (GE Silent, USA) with an 18-channel body coil. The protocol of MRI for prostate examination is summarized in Table 1.

Post-processing of IVIM was performed using software based on AW workstation (GE Silent, USA). The DWI data were calculated automatically with the following two models [5]:

1. Mono-exponential model (MEM)

$$S(b)/S(0) = \exp(-b \cdot ADC)$$

2. Bi-exponential model (BEM)

$$S(b)/S(0) = f \cdot \exp(-b \cdot D^*) + (1-f) \cdot \exp(-b \cdot D)$$

In the above formula, *S(b)* is the signal intensity at a specific b-value and $S(0)$ is the signal intensity when b= 0 s/mm^2. ADC is the diffusion coefficient of the conventional mono-exponential model. *D*, D^*, and f are quantitative parameters which fitted with the bi-exponential model. *D* is the pure molecular

diffusion coefficient, D^* is the perfusion-related diffusion coefficient, and f is the perfusion fraction.

Diseased region were manually outlined around the whole lesion on all slices of DWI images by two radiologists (with four and five years of experience with prostate MRI) in consensus, and using T_2WI and ADC map as references. Both radiologists were blinded to the RP results. Finally, ADC, ADC_{slow}, ADC_{fast}, $ADC_{standard}$ and F_{fast} were got from workstation automatically after the manual measuring (Figure.2).

Table 1 MRI protocol for prostate examination

Sequence	T_1WI	T_2WI (axial, sagittal, coronal)	DWI	IVIM
Repetition time (ms)	550	3600-4100	2500	2500
Echo time (ms)	8	78	70	70
Slice thickness (ms)	4	4	4	4
Slice gap (ms)	0	0	0	0
Slices	25	23	22	22
Field of view (mm2)	260×320	260×320	260×320	260×320
Matrix	320×320	320×320	320×320	320×320
Flip angle (degree)	160	160	90	90
Temporal resolution (s)	NA	NA	NA	NA
b value (S/mm2)	NA	NA	0, 1000	0, 10, 20, 50, 70, 100, 200, 700, 1000
Average	1	1	4	1-10

(T_1WI, T_1-weighted imaging; T_2WI, T_2-weighted imaging; NA, not applicable.)

Quantitative analysis

One-way ANOVA analysis was used to evaluate the relationship between benign and malignant group. Receiver operating characteristic (ROC) curve analysis was applied to evaluate the diagnostic performance of each parameter for distinguishing between benign and malignant group. Diagnostic performance was expressed by the area under the ROC curve (AUC). SPSS 17.0 (Chicago, IL, USA) was used for statistical analysis. The significance level was set at $P < 0.05$ for all analyses.

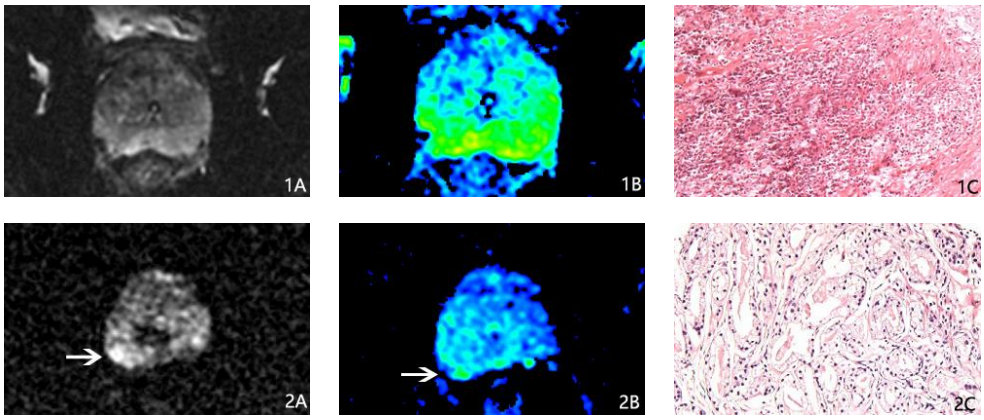

Fig 2 (1) A 64-year-old patient was confirmed to be prostatitis by pathology. (1A) DWI (b=800s/mm^2) and (1B) ADC_{slow} imaging (1C) pathologic imaging. (2) A 72-year-old patient was confirmed to be prostatic cancer by pathology. (1A) DWI imaging (b=800s/mm^2) and (1B) ADC_{slow} imaging show the tumor (white arrow) (1C) pathologic imagin

RESULTS

One-way ANOVA analysis results

One hundred and twenty four patients (with a mean age of 67.4 years; range, 48-81 years) were included (Figure.1), including cancer (n = 47), Benign Prostatic Hyperplasia (n = 4), prostatitis (n = 4) and prostatitis with hyperplasia(n = 30). There were significant differences in ADC_{slow}, ADC_{fast}, $ADC_{standard}$, F_{fast}

and ADC value between the two groups ($P < 0.05$). All the parameters between benign and malignant group are shown in Table 2.

Table 2 Comparison of the parameters between benign and malignant group

Parameter	Benign lesion group	Malignant lesion group	F value	*P* value
ADC ($\times 10^{-3}$ mm^2/s)	1.222-1.289	0.727-0.859	193.082	0.000
	(1.255 ±0.146)	(0.793 ±0.225)		
ADC_{slow} ($\times 10^{-3}$ mm^2/s)	0.432-0.453	0.292-0.312	330.532	0.000
	(0.442 ±0.045)	(0.302 ±0.034)		
ADC_{fast} ($\times 10^{-3}$mm^2/s)	0.681-0.763	0.374-0.412	112.844	0.000
	(0.722 ±0.182)	(0.430 ±0.063)		
$ADC_{standard}$ ($\times 10^{-3}$ mm^2/s)	3.714-4.911	13.968-26.699	102.123	0.000
	(4.312 ±2.637)	(20.333 ±3.162)		
F_{fast}	0.569-0.603	0.275-0.333	324.304	0.000
	(0.586 ±0.075)	(0.304 ±0.098)		

The ROC curve analyses of parameters

The results of the ROC curve analyses of parameters are reported in Table 3 and Figure.3. Among the table and ROC couve, ADC_{slow}, F and ADC_{fast} provided better sensitivity compared to ADC, and ADC_{fast} provided better specificity compared to ADC. ADC_{slow}, F and ADC_{fast} showed higher AUCs than ADC. While the $ADC_{standard}$ showed lower AUCs than ADC ($P > 0.05$ for all comparisons).

Table 3 Comparison of the ROC curve of parameters in MEM and BEM

Paremeter	AUC	Youden index	Optimal threshold ($\times 10^{-3}$mm^2/s)	Sensitivity (%)	Specificity (%)
ADC_{fast}	0.996	0.953	0.536	97.4	97.9
ADC_{slow}	0.997	0.953	0.369	97.4	95.7
F	0.984	0.837	0.476	93.5	91.5
ADC	0.98	0.818	1.115	80.1	95.7
$ADC_{standard}$	0.911	0.759	4.925	84.4	91.5

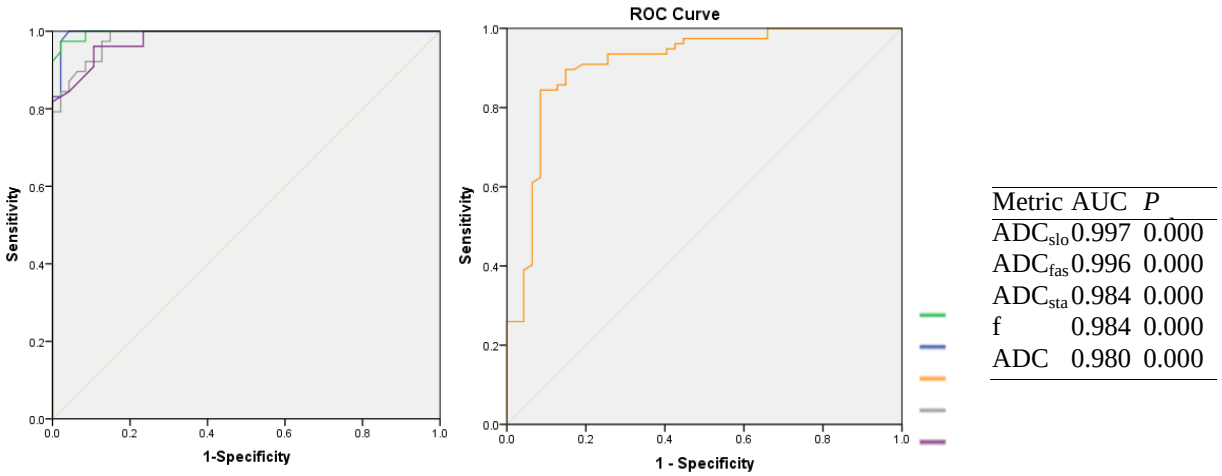

Fig 3 ROC curves of the parameters, including ADC_{fast} (blue line), ADC_{slow} (green line), f (gray line), ADC (purple line), and $ADC_{standard}$ (yellow line). The AUC and *P* value for each parameter are shown in the lower right corner.

DISCUSSION

DWI has been taken for granted as an important sequence of MRI for making a definite diagnosis in Prostatic lesions [6].Water diffusion behavior in biologic tissues is more complicated than completely free water diffusion. According to the theory of IVIM, signal acquired by DWI includes two forms of

microscopic motion. The one is the motion of water molecules and other is blood microcirculation in capillary network. Some study show that the IVIM based on bi-exponential model provides more quantitative parameters about the complicated diffusion behavior of water molecules [7]. ADC value derived from the bi-exponential model is highly correlated with cell density in biological tissues [8]. Some researchers' use the bi-exponential model in the evaluation of PCa [9], and the study show that bi-exponential model is better than the mono-exponential model [10]. Hence, IVIM based on bi-exponentia model was selected as our research method in differential diagnosis of benign prostate lesions and prostatic cancer. In our study, all metrics in Benign lesion group were significantly different from those in Malignant lesion Group. These results were consistent with previous studies [11].

ROC curves of the parameters, including ADC_{fast} (blue line), ADC_{slow} (green line), f (gray line), ADC (purple line), and $ADC_{standard}$ (yellow line). The AUC and p value for each parameter are shown in the lower right corner. By the ROC curve analyses. The role of ADC_{fast} and ADC_{slow} in the differential diagnosis of benign and malignant tumors has been extensively demonstrated in different organs in vivo [12]. The study conducted by C Schmid Tannwald revealed that ADC_{fast} and ADC_{slow} value strongly suggests a malignant leisons. The ADC_{fast} and ADC_{slow} were useful in the differentiation between benign and cancerous tissues. There were also other reports about the parameters of IVIM, which showed significant differences between maligant lesions and benign lesions [13]. Because an increase in cell density and the nucleus will be resulted in a decreased intercellular space, which highly restricts water molecule motion in malignant lesions, in which the ADC_{fast} and ADC_{slow} value was proportional to the mean capillary segment length and average blood velocity. We found that the f values of malignant lesions were significantly lower, than the benign lesions and prostatic cancer. Malagi concluded that the f values of normal tissues were significantly greater than that of invasive carcinomas [14]. Furthermore, F values resulted from the high cellularity of tumor tissues, and these always corresponded with lower conventional ADC values. The F value also may correlate with the amount of normal angiogenesis with intact vessels in terms of basement membrane thickness and pericyte coverage. A study of sorafenib treatment in advanced hepatocellular carcinoma (HCC) revealed that advanced HCC cases had a lower f value, when compared with normal liver [15]. Jha P concluded that the f value in pancreatic cancer was markedly reduced, when compared with healthy pancreatic tissues [16]. It could be speculated that the decreased f value resulted from the microvascular compression caused by the highly increased cell density in malignant lesions. There was seldom report about the effect of the $ADC_{standard}$. We found that $ADC_{standard}$ had lower Youden index than the ADC. According to the ROC curves, the diagnostic efficacy of $ADC_{standard}$ is lower than the ADC, which is different from other paremeters derived from IVIM. So this tissue requires further investigation.

However, our present study has several limitations. At first, the patient population was relatively small. Secondly, the homogeneity in prostate malignant and benign lesions, and it may cause the lower AUC of the parameters from different diffusion models. We intend to make further investigate about the ability of the mono-exponential and bi-exponentialmodels.

COMPETING INTERESTS

The authors declare that they have no conflicts of interest.

ACKNOWLEDGMENTS

This work was supported by Medical science fund of Guangdong Province, China (Grant No.2016118164716276).

REFERENCES

[1]. Glazer, I. D, Hassanzadeh, Elmira, Fedorov, Andriy, et al. Diffusion-weighted endorectal MR imaging at 3T for prostate cancer: correlation with tumor cell density and percentage Gleason pattern on whole mount pathology. Abdom Radiol (NY), 2017, 42(3):918-925. Doi: 10.1007/s00261-016-0942-1.

[2]. Malagi AV, Das CJ, Khare K, Calamante F, Mehndiratta A. Effect of combination and number of b values in IVIM analysis with post-processing methodology: simulation and clinical study. MAGMA, 2019, 32(5):519-527. Doi: 10.1007/s10334-019-00764-0.

[3]. Kang KM, Lee JM, Yoon JH, Kiefer B, Han JK, Choi BI. Intravoxel incoherent motion diffusion-weighted MR imaging for characterization of focal pancreatic lesions. Radiology, 2014, 270(2): 444-453. Doi: 10.1148/radiol.13122712.

[4]. Kartalis N, Manikis GC, Loizou L, Albiin N, Zollner FG, Del CM, et al. Diffusion-weighted MR imaging of pancreatic cancer: A comparison of mono-exponential, bi-exponential and non-Gaussian kurtosis models. Eur J Radiol Open. 2016, 3:79-85. Doi: 10.1016/j.ejro.2016.04.002.

[5]. Zhang P, Min X, Wang L, Feng Z, Ke Z, You H, et al. Bi-exponential versus mono-exponential diffusion-weighted imaging for evaluating prostate cancer aggressiveness after radical prostatectomy: a whole-tumor histogram analysis. Acta Radiol, 2019, 284185119837932. Doi: 10.1177/0284185119837932.

[6]. Ma XZ, Lv K, Sheng JL, Yu YX, Pang PP, Xu MS, et al. Application evaluation of DCE-MRI combined with quantitative analysis of DWI for the diagnosis of prostate cancer. Oncol lett, 2019, 17(3):3077-3084. Doi: 10.3892/ol.2019.9988.

[7]. Kayal EB, Kandasamy D, Khare K, Alampally JT, Bakhshi S, Sharma R, Mehndiratta A. Quantitative Analysis of Intravoxel Incoherent Motion (IVIM) Diffusion MRI using Total Variation and Huber Penalty Function. Med Phys, 2017, 44(11):5849-5858. Doi: 10.1002/mp.12520.

[8]. Xu Y, Xu Q, Sun H, Liu T, Shi K, Wang W. Could IVIM and ADC help in predicting the KRAS status in patients with rectal cancer? Eur Radiol, 2018, 28(7):3059-3065. Doi: 10.1007/s00330-018-5329-y.

[9]. Zhang P, Min X, Wang L, Feng Z, Ke Z, You H, et al. Bi-exponential versus mono-exponential diffusion-weighted imaging for evaluating prostate cancer aggressiveness after radical prostatectomy: a whole-tumor histogram analysis. Acta Radiol, 2019, 284185119837932. Doi: 10.1177/0284185119837932.

[10]. Karunamuni RA, Kuperman J, Seibert TM, Schenker N, Rakow-Penner R, Sundar VS, et al. Relationship between kurtosis and bi-exponential characterization of high b-value diffusion-weighted imaging: application to prostate cancer. Acta Radiol, 2018, 59(12):1523-1529. Doi: 10.1177/0284185118770889.

[11]. Shan Y, Chen X, Liu K, Zeng M, Zhou J. Prostate cancer aggressive prediction: preponderant diagnostic performances of intravoxel incoherent motion (IVIM) imaging and diffusion kurtosis imaging (DKI) beyond ADC at 3.0 T scanner with gleason score at final pathology. Abdom Radiol (NY), 2019, 44(10):3441-3452. Doi: 10.1007/s00261-019-02075-3.

[12]. Naganawa S, Sato C, Kumada H, Ishigaki T, Miura S, Takizawa O. Apparent diffusion coefficient in cervical cancer of the uterus: comparison with the normal uterine cervix. Eur Radiol, 2005, 15(1):71-78. Doi: 10.1007/s00330-004-2529-4.

[13]. Yang DM, Kim HC, Kim SW, Jahng GH, Won KY, Lim SJ, Oh JH. Prostate cancer: correlation of intravoxel incoherent motion MR parameters with Gleason score. Clin Imaging. 2016 May-Jun; 40(3):445-50. Doi: 10.1016/j.clinimag.2016.01.001.

[14]. Park HJ, Sung YS, Lee SS, Lee Y, Cheong H, Kim YJ, Lee MG. Intravoxel incoherent motion diffusion-weighted MRI of the abdomen: The effect of fitting algorithms on the accuracy and reliability of the parameters. J Magn Reson Imaging, 45(6):1637-1647. Doi: 10.1002/jmri.25535.

[15]. Jeon TY, Kim CK, Kim JH, Im GH, Park BK, Lee JH. Assessment of early therapeutic response to sorafenib in renal cell carcinoma xenografts by dynamic contrast-enhanced and diffusion-weighted MR imaging. Br J Radiol, 2015, 88(1053):20150163. Doi: 10.1259/bjr.20150163.

[16]. Jha P, Yeh BM, Zagoria R, Collisson E, Wang ZJ. The Role of MR Imaging in Pancreatic Cancer. Magn Reson Imaging Clin N Am, 2018, 26(3):363-373. Doi: 10.1016/j.mric.2018.03.004.